CALCULATIONS ON THE STRUCTURES OF MnB_9 CLUSTERS AND ITS INTERACTION WITH H_2

Phan Trung Cang[1], Ho Sy Linh[2], Nguyen Minh Thao[3,4,5*], Ho Sy Thang[6], and Bui Tho Thanh[4]

[1]IT and Lab Center, Dong Thap University, Vietnam

[2]Faculty of Natural Sciences Teacher Education, Dong Thap University, Vietnam

[3]Research Affairs Office, Dong Thap University, Vietnam

[4]Faculty of Chemistry, University of Science, VNU-HCM, Vietnam

[5]Vietnam National University Ho Chi Minh City, Vietnam

[6]Graduate Studies Office, Dong Thap University, Vietnam

[*]Corresponding author: Nguyen Minh Thao, Email: nmthao@dthu.edu.vn

Article history

Received: 06/01/2022; Received in revised form: 24/3/2022; Accepted: 17/5/2022

Abstract

The structures of the MnB_9 cluster have been investigated by the theoretical calculations. The combination of the genetic algorithm and the density functional theory calculations (GA-DFT) find out seventeen minimum structures, including the local minimum structures and the global minimum structure. The MnB_9 cluster can be formed by adding an Mn atom into the B_9 cluster. There is also a strong interaction between the MnB_9 cluster and the H_2 molecule resulting in the expansion or dissociation of the H-H bond. This demonstrates the potential applicability of boron clusters doping manganese in the field of catalyst and adsorption.

Keywords: *GA-DFT, optimization, density functional theory, MnB_9.*

DOI: https://doi.org/10.52714/dthu.12.5.2023.1077

Cite: Phan, T. C., Ho, S. L., Nguyen, M. T., Ho, S. T., & Bui, T. T. (2023). Calculations on the structures of MnB_9 clusters and its interaction with H_2. *Dong Thap University Journal of Science, 12*(5), 101-110. https://doi.org/10.52714/dthu.12.5.2023.1077

TÍNH TOÁN CẤU TRÚC CỦA CÁC CLUSTER MnB_9 VÀ SỰ TƯƠNG TÁC VỚI H_2

Phan Trung Cang[1], Hồ Sỹ Linh[2], Nguyễn Minh Thảo[3,4,5*], Hồ Sỹ Thắng[5] và Bùi Thọ Thanh[4]

[1]Trung tâm Thực hành - Thí nghiệm, Trường Đại học Đồng Tháp, Việt Nam

[2]Khoa Sư phạm Khoa học tự nhiên, Trường Đại học Đồng Tháp, Việt Nam

[3]Phòng Khoa học và Công nghệ, Trường Đại học Đồng Tháp, Việt Nam

[4]Khoa Hóa học, Trường Đại học Khoa học Tự nhiên, ĐHQG-HCM, Việt Nam

[5]Đại học Quốc gia thành phố Hồ Chí Minh, Việt Nam

[6]Phòng Đào tạo Sau đại học, Trường Đại học Đồng Tháp, Việt Nam

[*]Tác giả liên hệ: Nguyễn Minh Thảo, Email: nmthao@dthu.edu.vn

Lịch sử bài báo

Ngày nhận: 06/01/2022; Ngày nhận chỉnh sửa: 24/3/2022; Ngày chấp nhận: 17/5/2022

Tóm tắt

Cấu trúc của cụm nguyên tử MnB_9 được nghiên cứu bằng các tính toán lý thuyết. Sự kết hợp của giải thuật di truyền với tính toán lý thuyết phiếm hàm mật độ tìm kiếm được 17 cấu trúc cực tiểu bao gồm cấu trúc cực tiểu cục bộ và cấu trúc cực tiểu toàn bộ. Cụm nguyên tử MnB_9 có thể được hình thành bằng cách thêm một nguyên tử Mn vào cụm nguyên tử B_9. Cụm nguyên tử MnB_9 tương tác mạnh với phân tử H_2, làm kéo giãn liên kết hoặc phân ly liên kết H-H. Điều đó cho thấy khả năng ứng dụng cụm nguyên tử boron pha tạp manganese trong lĩnh vực xúc tác và hấp phụ.

Từ khóa: *GA-DFT, sự tối ưu hóa, lý thuyết phiếm hàm mật độ, MnB_9.*

1. Introduction

Boron is widely investigated because of its applications as superhard materials, semiconductor materials, anti-cancer drugs, (Alexandrova, 2006; Shakerzadeh et al., 2019). For lacking electronics in the valence shell ($2s^2 2p^1$), boron can create a bond with different atoms to stablize the valence shell. Boron cluster structures are planar, near planar, or tube shape (Alexandrova, 2006; Liu et al., 2007; Shakerzadeh et al., 2019). Doping the transition metal as Sc, Ti, V, Cr, Mn, Fe, and Au can form different structures and properties (Huynh et al., 2018; Jia et al.; 2013, Liu et al., 2007; Nguyen & Bui, 2022; Nguyen et al., 2019; Nguyen et al., 2021; Tran et al., 2019; Tran et al., 2020).

Hydrogen has been interested in the area of energy research. Hydrogen storage as gas or liquid has potential problems of safety, cost, and capacity. Therefore, industrial applications of hydrogen depend on their storage. Nowadays, solid materials attract many researchers. Theoretical and experimental studies show that transition metal doped-boron cluster can store hydrogen (Jia, 2014; Kumar et al., 2020; Kuraganti et al., 2019; Ray et al., 2019; Rydén et al., 2013).

This study investigated MnB_9 cluster's global and local minimum structures by the evolutional algorithm and quantum calculations. Interactions between MnB_9 and H_2 have also been performed to find out their potential application.

2. Methods

The genetic algorithm and density functional theory (GA-DFT) were used to study global and local structures on the potential surface energy. The USPEX 10.3 code performed the genetic algorithm (Lyakhov et al., 2013; Oganov & Glass, 2006; Oganov et al., 2011) and the Quantum Espresso 6.0 (Giannozzi, 2009) calculated the energy value of cluster in the optimization. The GA process includes many generations. In the first generation, clusters were randomly created. Based on the energy, some structures were kept to form the next generation. Besides that, the different clusters were born by mutation, crossing, and random. The GA-DFT process was repeated to gain the stop condition.

After the GA-DFT calculations were finished, all structures were reoptimized by the PBE0 functional (Jian et al., 2016; Zhao et al., 2017). To save the computational cost, the def2-SVP basis set was first used. From the obtained structures and their energy, optimization was reoptimized with the def2-TZVP basis set. Different multiplicities were set to determine the electronic state of low energy. The DFT calculations were done by the ORCA 4.2.1 (Neese, 2012). In addition, some structures were built to obtain more the local minimum. To assure that the clusters were optimized at the minimum of potential energy surface (PES), we performed frequency calculations of all clusters at the same level of theory and no negative frequency for any clusters was found. The zero-point energies (ZPEs) were used to get the relative energies.

To study MnB_9 cluster - H_2 molecule interactions, low-energy structures were used. The initial interaction structures were randomly created by the put H_2 around the surface of the MnB_9 isomers at many positions. After that, these structures were respectively optimized at the PBE0/def2-SVP and the PBE0/def2-TZVP. The harmonic vibrational frequency was calculated at the PBE0/def2-TZVP level to determine the minima structures. The zero-point energy was also used in calculating the relative energy.

3. Results and discussion

3.1. The isomer structures of the MnB_9 cluster

The structure, symmetry, electronic state, relative energy, and harmonic vibrational frequencies of the isomers of the MnB_9 cluster are presented in Figure 1 and Table 1. The harmonic vibrational frequency values at the PBE0/def2-TZVP level of all structures in Table 1 are positive. They show that these structures are at the minima on the potential energy surface.

Based on the results of the density functional theory calculations with the PBE0 functional and the def2-TZVP basis set, the structure N1 with the C_s symmetry is the most stable isomer of the MnB_9 cluster. The electronic state of this global structure is the $^5A'$ state. Three isomers of N2, N3, and N4 have the relative energies of 0.20, 0.29, and 0.45 eV, respectively. These electronic states of three local structures are also $^5A'$ state. The five next isomers of N5, N6, N7, N8, and N9 are less stable than the global

structure N1 from 0.75 eV to 1.14 eV. The symmetry of N6 and N9 are both C_s with the $^5A''$ electronic states while the symmetry of N5, N7, and N8 are C_1 symmetry. The isomer N10 is higher in energy than isomer N9 by 0.58 eV. Three isomers N11, N12, and N13 have structures with the C_s symmetry. These four isomers N10 - N14 are near degeneracy in energy. The electronic states of N11 and N12 are $^5A''$ states while that of N13 is $^5A'$ state. The isomer N14 have the $^5A_2$ electronic state in C_{2v} symmetry which is bigger than the global minimum structure by 1.97 eV. The relative energies of N15, N16, and N17 isomers are 2.18, 3.14, and 3.53 eV, respectively. All structures have low energy electronic states at the high multiplicity of 5. This is the characteristic property of the electronic state of the compounds containing manganese element of the open-shell valance containing 5 electrons in 3d orbital.

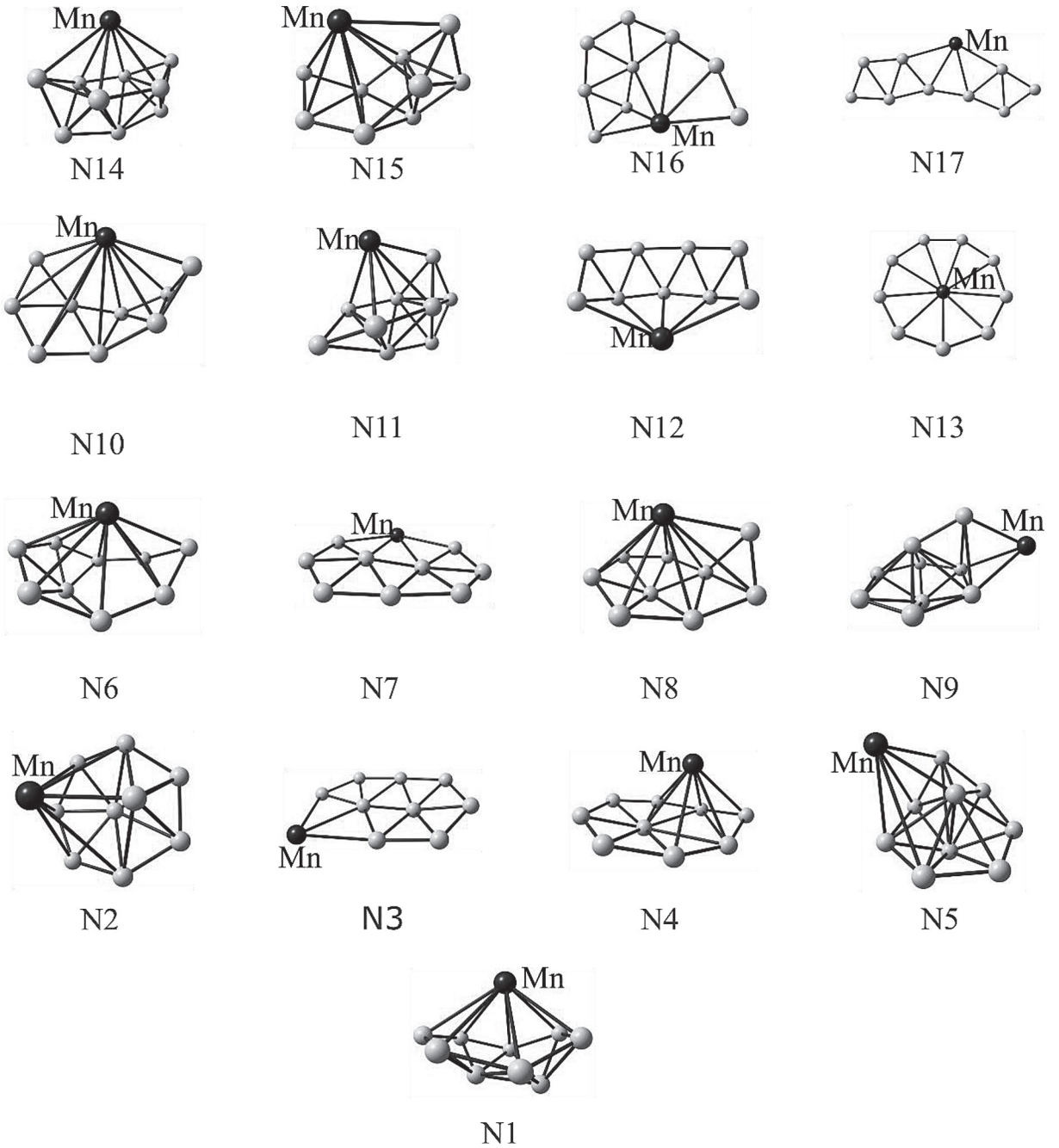

Figure 1. The structure of MnB_9 cluster

Table 1. The structure, symmetry, electronic state, relative energy, and harmonic vibrational frequencies of the isomers of MnB_9 cluster at PBE0/def2-TZVP level

Isomer	Sym.	State	RE	Harmonic vibrational frequencies (cm^{-1})
N1	C_s	$^5A'$	0.00	189.40; 246.81; 283.82; 354.27; 373.91; 375.64; 450.12; 471.61; 490.54; 513.42; 578.84; 630.25; 665.95; 713.70; 766.62; 794.80; 861.77; 923.46; 1026.83; 1084.40; 1122.33; 1142.02; 1208.56; 1223.44
N2	C_s	$^5A'$	0.20	108.56; 122.85; 246.68; 249.68; 282.16; 333.84; 386.93; 413.81; 426.53; 496.64; 527.45; 582.31; 612.47; 627.16; 731.76; 737.01; 760.71; 865.68; 989.53; 1007.15; 1215.38; 1216.74; 1329.45; 1337.34
N3	C_s	$^5A'$	0.29	73.83; 168.11; 215.82; 234.90; 291.31; 324.43; 376.60; 415.60; 483.32; 487.07; 514.51; 562.23; 628.66; 705.13; 643.57; 786.27; 880.14; 921.57; 1067.41; 1124.92; 1135.62; 1233.86; 1237.90; 1319.08
N4	C_s	$^5A'$	0.45	67.07; 132.99; 210.65; 238.89; 247.48; 346.23; 365.13; 386.23; 455.94; 475.34; 483.30; 513.07; 581.92; 676.64; 686.56; 689.88; 791.61; 900.02; 988.51; 1116.26; 1184.25; 1280.35; 1404.78; 1450.42
N5	C_1	^5A	0.66	116.83; 156.19; 177.69; 308.17; 322.83; 350.04; 383.05; 427.32; 447.77; 505.05; 555.30; 567.60; 610.24; 631.87; 696.90; 757.64; 816.11; 893.24; 912.70; 1009.12; 1098.24; 1211.73; 1299.88; 1373.85
N6	C_s	$^5A''$	0.75	170.52; 228.16; 247.46; 253.13; 279.04; 315.28; 344.39; 415.62; 463.77; 470.17; 509.38; 568.38; 616.22; 669.92; 701.37; 711.08; 804.14; 889.24; 1016.12; 1088.96; 1222.41; 1282.32; 1343.85; 1378.39
N7	C_1	^5A	0.82	98.22; 143.88; 205.15; 223.19; 311.88; 330.23; 362.96; 424.17; 441.33; 454.26; 485.21; 531.66; 600.30; 658.18; 664.58; 782.25; 831.30; 882.02; 1024.68; 1052.09; 1156.65; 1184.88; 1296.78; 1354.77
N8	C_1	^5A	1.07	66.72; 162.15; 225.77; 250.89; 282.35; 352.31; 384.50; 436.61; 452.14; 477.01; 529.73; 560.90; 596.08; 609.31; 695.90; 772.22; 783.42; 897.26; 1042.11; 1070.23; 1182.66; 1206.50; 1263.70; 1311.98
N9	C_s	$^5A''$	1.14	179.96; 203.33; 203.57; 268.08; 306.69; 369.14; 421.30; 448.44; 468.56; 469.31; 558.62; 604.97; 622.49; 665.29; 670.51; 744.12; 817.38; 900.21; 957.89; 1026.74; 1112.18; 1185.40; 1216.85; 1263.51
N10	C_1	^5A	1.72	83.29; 176.67; 184.73; 282.86; 316.73; 347.73; 367.67; 387.72; 446.53; 474.79; 483.90; 554.22; 602.98; 618.78; 636.05; 680.54; 763.17; 871.84; 1037.94; 1058.64; 1162.56; 1205.27; 1258.26; 1315.79

Isomer	Sym.	State	RE	Harmonic vibrational frequencies (cm^{-1})
N11	C_s	$^5A''$	1.77	190.44; 225.84; 292.16; 317,80; 321.94; 395.34; 400.26; 451.94; 460.93; 465.60; 501.09; 526.13; 607.72; 638.33; 642.37; 694.89; 815.82; 888.95; 899.99; 1003.55; 1050.68; 1096.10; 1143.39; 1232.36
N12	C_s	$^5A''$	1.80	142.35; 173.70; 225.26; 288.06; 289.98; 354.46; 372.67; 411.11; 467.45; 541.32; 544.02; 601.58; 660.22; 678.92; 680.09; 726.08; 811.37; 870.40; 1052.70; 1056.12; 1163.43; 1186.97; 1213.17; 1257.93
N13	C_s	$^5A'$	1.85	65.70; 103.62; 176.69; 231.52; 278.08; 306.43; 309.41; 348.42; 348.99; 446.16; 448.95; 464.06; 464.75; 542.20; 542.60; 630.37; 767.59; 809.62; 1009.72; 1109.35; 1245.94; 1250.95; 1562.71; 1569.21
N14	C_{2v}	$^5A_2$	1.97	156.02; 212.99; 265.01; 304.79; 314.81; 329.51; 342.55; 420.77; 442.14; 443.92; 631.34; 637.36; 658.09; 681.39; 696.83; 771.41; 773.09; 859.38; 885.33; 934.88; 1030.13; 1131.70; 1162.06; 1219.93
N15	C_1	^5A	2.18	163.96; 179.04; 234.33; 311.07; 320.33; 371.14; 389.91; 463.37; 516.67; 523.35; 538.99; 594.39; 597.27; 631.85; 653.45; 698.46; 756.08; 819.85; 881.66; 992.97; 1058.78; 1072.89; 1148.62; 1291.92
N16	C_1	^5A	3.14	96.40; 114.18; 135.86; 186.22; 248.61; 293.62; 343.33; 380.72; 412.22; 441.11; 467.23; 475.73; 500.91; 568.30; 620.92; 695.84; 743.18; 837.20; 964.60; 1120.28; 1183.24; 1268.35; 1326.37; 1461.01
N17	C_s	$^5A''$	3.53	14.44; 77.44; 154.56; 160.40; 180.49; 218.88; 322.26; 349.51; 362.80; 418.19; 467.65; 473.06; 568.73; 659.72; 691.39; 781.67; 967.93; 1072.47; 1097.18; 1161.04; 1256.98; 1336.42; 1351.29

3.2. The interaction between MnB_9 cluster and H_2 molecule

The H_2 molecule is optimized at the PBE0/def2-TZVP level. The obtained results include the bond length, the bond energy, and the zero-point energy (ZPE) of the H_2 molecule in Table 3. This bond length is 0.746 Å by the PBE0/def2-TZVP level. This value from the experiment is 0.741 Å. The bond energy of H_2 is 4.52 eV and this value in the different report is 4.55 eV. The ZPE value of the H_2 molecule is 0.274 eV, which is in line with those in different reports (Tran & Nguyen, 2020). The above results show that the PBE0/def2-TZVP level is suitable in this study.

Table 3. The bond length (L_{H-H}) and the bond energy (E_b), and the zero-point energy (ZPE) of H_2

Parameter	PBE0/def2-TZVP	Reference
L_{H-H} (Å)	0.746	0.741 (Kumar, A. et al., 2020)
E_b (eV)	4.52	4.55 (Kumar, A. et al., 2020); 4.525 (Tran, T. T. H. and Nguyen, V. H., 2020);
ZPE (eV)	0. 274	0.269 (Tran, T. T. H. and Nguyen, V. H., 2020);

By the PBE0 optimizations, many minimal structures of the MnB_9-H_2 cluster are obtained. They include the structures with and without the dissociate H-H bond. In this study, the structures with the dissociate H-H bond have the relative energy values from 0.00 eV to 2.07 eV at the PBE0/def2-TZVP level. The most stable structure without the dissociated H-H bond is higher than the most stable structure with the dissociated H-H bond by 2.77 eV. In this report, the structures which have the small different energy are presented by only one structure with the smallest energy structure.

The adsorption energy of H_2 on MnB_9 cluster is calculated by the following formula:

$$E_{ads\text{-}2H} = (E_{MnB9} + 2*E_H - E_{MnB9\text{-}H2})$$

$$E_{ads\text{-}H2} = (E_{MnB9} + E_{H2} - E_{MnB9\text{-}H2})$$

where $E_{ads\text{-}2H}$, $E_{ads\text{-}H2}$, E_{MnB9}, E_H, E_{H2}, and $E_{MnB9\text{-}H2}$ are the adsorption energy with the dissociated H-H bond, the adsorption energy without the dissociated H-H bond, the energies of MnB_9 cluster, H atom, H_2 molecule, and the MnB_9-H_2 complex, respectively.

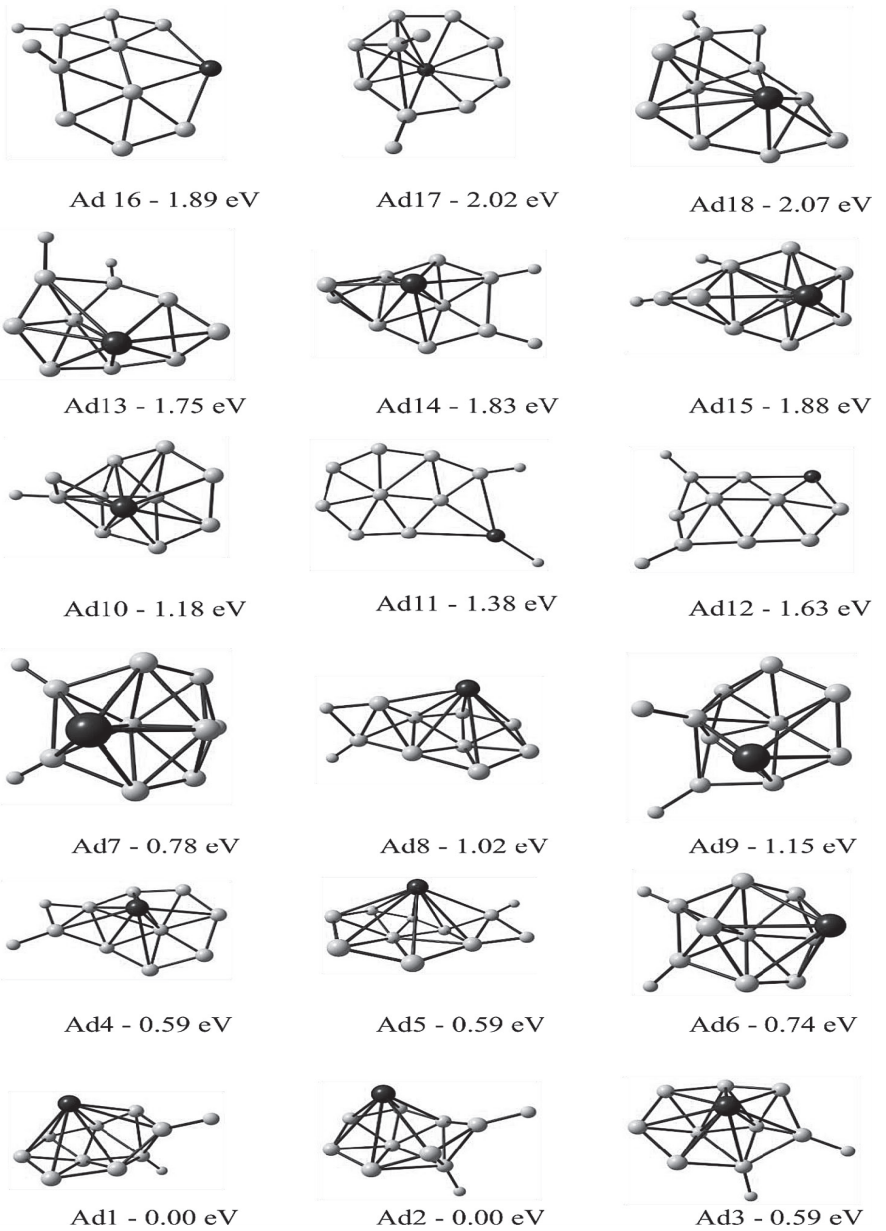

Figure 2. The interaction structures between MnB_9 and H_2 with the dissociated H-H bond

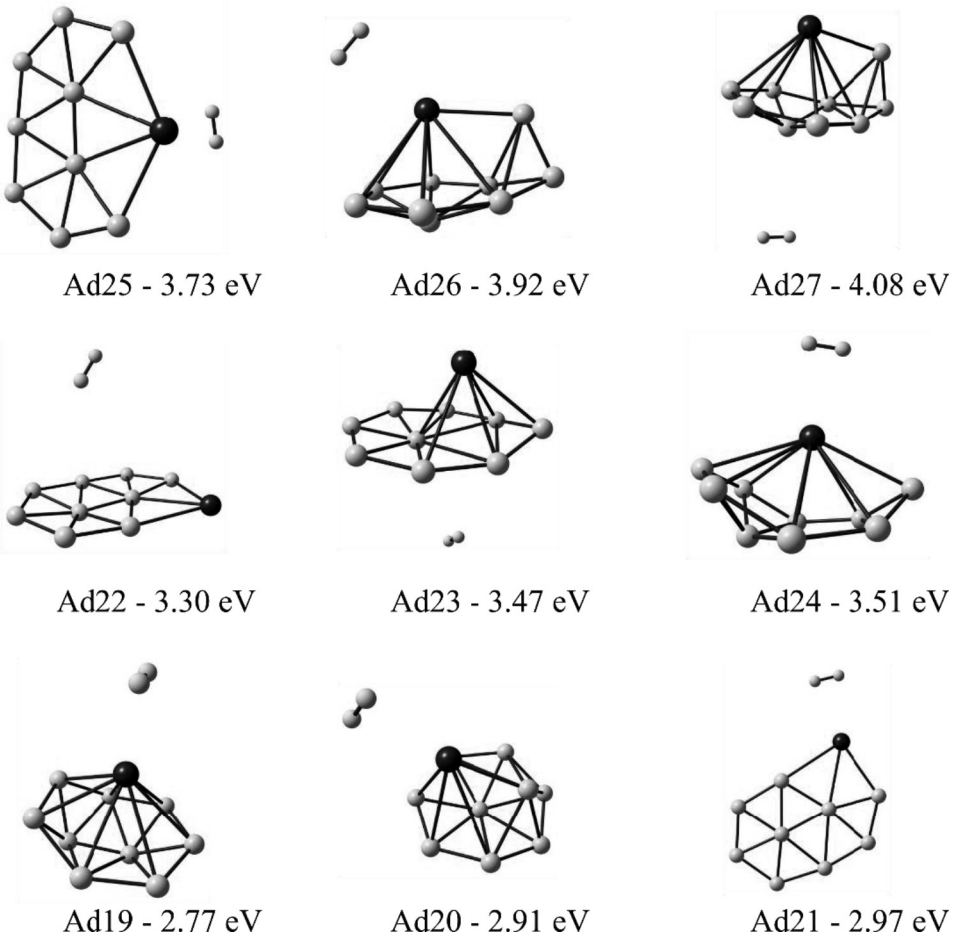

Figure 3. The interaction structures between MnB_9 and H_2 without the dissociated H-H bond

In Figure 2, eighteen structures with the dissociated H-H bond are presented. Like the observation in these structures, the H-H bond is dissociated belonging to the B-B bond, except that the Ad11 structure with the H-H bond is dissociated at the position of the Mn-B bond. It shows that the strong interaction between hydrogen and boron. Two structures that have the lowest energy are Ad1 and Ad2. The Ad1 structure is formed by the N1 isomer of the MnB_9 cluster with H_2, and the Ad2 structure is formed between the N5 isomer of the MnB_9 cluster and H_2.

The H_2 molecule is not dissociated around the Mn atom. The energy of the structure Ad19 is higher than the most stable structure with the dissociated H-H bond by 2.77 eV. Two structures of Ad20 and Ad21 are higher in energy than structure Ad19 by 0.14 eV and 0.20 eV, respectively. The others as Ad22, Ad23, and Ad25 are less stable in energy than Ad19 by 0.53, 0.70, and 1.31 eV, respectively. In three structures, the H_2 molecules are near the surface of boron than manganese. Some different structures have high energy as Ad24, Ad25, and Ad26 with H_2 near the Mn atom.

Table 4. The distance between two hydrogen atom (D_{H-H}) and adsorption energy (E_{ads}) of H_2 molecule

Structure	D_{H-H} (Å)	E_{ads} (eV)
Ad1	3.49	0.29
Ad19	0.76	0.11

The Ad1 and Ad19 are two interaction structures of H_2 and isomer N1 of the MnB_9 cluster. In structure Ad1, the bond length of the H-H bond is dissociated into two atoms with a distance of 3.49 Å. The chemisorption energy of this process is 0.29 eV. The bond length of the H-H bond in structure Ad19 is expanded to 0.76 Å from 0.746 Å at the optimized

geometry of the H_2 molecule at PBE0/def2-TZVP level. It indicates that the bond between two H atoms has been decreased. The adsorption of H_2 on the structure Ad19 is 0.11 eV. The average physisorption energy of Mg_2B_9 is 0.16 eV (Kumar, A. et al., 2020). All the above results show that the MnB_9 cluster can interact with H_2 by chemisorption and physisorption.

4. Conclusion

The structures of the MnB_9 cluster and their interaction with hydrogen have been performed by the theoretical calculation. The seventeen structures of the MnB_9 cluster are obtained. The global minimum structure has the C_s symmetry. The MnB_9 cluster can be formed by adding one Mn atom to the B_9 cluster. The MnB_9 cluster can strongly interact with hydrogen molecule. In the interaction process, the H-H bond can be expanded or can be dissociated that show the potential of the MnB_9 cluster in the field of catalyst and adsorption./.

Acknowledgement: This research is supported by the project SPD2021.01.33, Dong Thap University.

References

Alexandrova, A. N., Boldyrev, A. I., Zhai, H.-J., & Wang, L.-S. (2006). All-boron aromatic clusters as potential new inorganic ligands and building blocks in chemistry. *Coordination Chemistry Reviews, 250*(21–22), 2811-2866. https://doi.org/10.1016/j.ccr.2006.03.032.

Giannozzi, P., Baroni, S., Bonini, N., Calandra, M., Car, R., Cavazzoni, C., Ceresoli, D., Chiarotti, G. L., Cococcioni, M., Dabo, I., Dal Corso, A., de Gironcoli, S., Fabris, S., Fratesi, G., Gebauer, R., Gerstmann, U., Gougoussis, C., Kokalj, A., Lazzeri, M., Martin-Samos, L., Marzari, N., Mauri, F., Mazzarello, R., Paolini, S., Pasquarello, A., Paulatto, L., Sbraccia, C., Scandolo, S., Sclauzero, G., Seitsonen, A. P., Smogunov, A., Umari, P., & Wentzcovitch, R. M. (2009). QUANTUM ESPRESSO: a modular and open-source software project for quantum simulations of materials. *Journal of Physics: Condensed Matter, 21*(39), 395502. https://doi.org/10.1088/0953-8984/21/39/395502.

Huynh, B. P. H., Nguyen, M. T., Phan, T. C., Tran, Q. T., & Tran, V. T. (2018). An investigation of the geometrical and electronic structures of MnB0/−/+ clusters by multiconfigurational CASSCF/CASPT2 method. *Dong Thap University Journal of Science, 30*, 95-101. https://doi.org/10.52714/dthu.30.2.2018.557.

Jia, J., Li, X., Li, Y., Ma, L., & Wu, H.-S. (2014). Density functional theory investigation on the structure and stability of Sc2Bn (n=1–10) clusters. *Computational and Theoretical Chemistry, 1027*, 128-134. https://doi.org/10.1016/j.comptc.2013.11.008.

Jia, J., Ma, L., Wang, J.-F., & Wu, H.-S. (2013). Structures and stabilities of ScBn (n = 1-12) clusters: an ab initio investigation. *Journal of Molecular Modeling, 19*(8), 3255-3261. https://doi.org/10.1007/s00894-013-1860-6.

Jian, T., Li, W.-L., Popov, I. A., Lopez, G. V., Chen, X., Boldyrev, A. I., Li, J., & Wang, L.-S. (2016). Manganese-centered tubular boron cluster - MnB16−: A new class of transition-metal molecules. *Journal of Chemical Physics, 144*(15), 154310. https://doi.org/10.1063/1.4946796.

Kumar, A., Vyas, N., & Ojha, A. K. (2020). Hydrogen storage in magnesium decorated boron clusters (Mg2Bn, n = 4–14): A density functional theory study. *International Journal of Hydrogen Energy, 45*(23), 12961-12971. https://doi.org/10.1016/j.ijhydene.2020.03.018.

Kuraganti, V., Jain, A., Bar-Ziv, R., Ramasubramaniam, A., & Bar-Sadan, M. (2019). Manganese doping of MoSe2 promotes active defect sites for hydrogen evolution. *ACS Applied Materials & Interfaces, 11*(28), 25155-25162. https://doi.org/10.1021/acsami.9b05670.

Liu, X., Zhao, G.-f., Guo, L.-j., Jing, Q., & Luo, Y.-h. (2007). Structural, electronic, and magnetic properties of MBn (M= Cr, Mn, Fe, Co, Ni, n≤7) clusters. *Physical Review A, 75*(6), 063201. https://doi.org/10.1103/PhysRevA.75.063201.

Lyakhov, A. O., Oganov, A. R., Stokes, H. T., & Zhu, Q. (2013). New developments in evolutionary structure prediction algorithm USPEX. *Computer Physics Communications, 184*(4), 1172-1182. https://doi.org/10.1016/j.cpc.2012.12.009.

Neese, F. (2012). The ORCA program system. Wiley Interdiscip. Rev. Comput. Mol. Sci, 2(1), 73-78.

Nguyen, M. T., & Bui, T. T. (2022). Study the structure, stability and CO2 adsorption of the ScVB5 cluster. *Vietnam Journal of Catalysis and Adsorption, 11*(1), 49-59. https://doi.org/10.51316/jca.2022.008.

Nguyen, M. T., Nguyen, T. H. H., Dang, T. T. L., Ly, H. H., Phan, T. C., Bui, V. T., Bui, T. T., Tran, Q. T., & Tran, V. T. (2019). The structural calculations of B40/-/+ and MnB30/-/+ clusters. *Vietnam Journal of Chemistry, 57*(6E1,2), 408-412.

Nguyen, M. T., Nguyen, T. N. T., Nguyen, T. L. H., & Bui, T. T. (2021). An investigation on the structures of Sc2B8 clusters by a combination of the genetic algorithm and density functional theory (GA-DFT) and its CO-adsorption. *Vietnam Journal of Catalysis and Adsorption, 10*(2), 65-71. https://doi.org/10.51316/jca.2021.030.

Oganov, A. R., & Glass, C. W. (2006). Crystal structure prediction using ab initio evolutionary techniques: principles and applications. *Journal of Chemical Physics, 124*(24), 244704. https://doi.org/10.1063/1.2210932.

Oganov, A. R., Lyakhov, A. O., & Valle, M. (2011). How evolutionary crystal structure prediction works - and why. *Accounts of Chemical Research, 44*(3), 227-237. https://doi.org/10.1021/ar1001318.

Ray, S. S., Sahoo, S. R., & Sahu, S. (2019). Hydrogen storage in scandium doped small boron clusters (BnSc2, n=3–10): A density functional study. *International Journal of Hydrogen Energy, 44*(12), 6019-6030. https://doi.org/10.1016/j.ijhydene.2018.12.109.

Rydén, J., Öberg, S., Heggie, M., Rayson, M., & Briddon, P. (2013). Hydrogen storage in the manganese containing metal–organic framework MOF-73. *Microporous and Mesoporous Materials, 165*, 205-209. https://doi.org/10.1016/j.micromeso.2012.08.024.

Shakerzadeh, E., Duong, V. L., Tahmasebi, E., & Nguyen, M. T. (2019). The scandium doped boron cluster B27Sc2+: a fruit can-like structure. *Physical Chemistry Chemical Physics, 21*(17), 8933-8939. https://doi.org/10.1039/C9CP00892F.

Tran, T. M. N., Nguyen, M. T., Tran, Q. T., & Tran, V. T. (2019). A CASSCF/CASPT2 MnB20/−/+. *Dong Thap University Journal of Science, 40*, 53-59. https://doi.org/10.52714/dthu.40.10.2019.733.

Tran, T. T. H., & Nguyen, V. H. (2020). Zero-point vibration of the adsorbed hydrogen on the Pt(110) surface. *Adsorption, 26*(3), 453-459. https://doi.org/10.1007/s10450-019-00195-2.

Tran, V. T., Ngo, T. P. A., Tran, T. T., Nguyen, T. H. H., Nguyen, M. T., Tran, Q. T., & Nguyen, H. L. (2020). Structures and properties of VB5−/0 clusters from density functional theory calculations. *Dong Thap University Journal of Science, 9*(5), 59-67. https://doi.org/10.52714/dthu.9.5.2020.818.

Zhao, L., Qu, X., Wang, Y., Lv, J., Zhang, L., Hu, Z., Gu, G., & Ma, Y. (2017). Effects of manganese doping on the structure evolution of small-sized boron clusters. *Journal of Physics: Condensed Matter, 29*(26), 265401. https://doi.org/10.1088/1361-648X/aa7190.